Spectrally Efficient FDM System with Probabilistic Shaping

Xinyue Liu and Izzat Darwazeh
Dept. of Electronic and Electrical Engineering
University College London
London WC1E 7JE, UK
{x.liu.17, i.darwazeh}@ucl.ac.uk

Nader Zein
NEC Laboratories Europe
NEC Europe
Middlesex HA4 6QE, UK
Nader.Zein@emea.nec.com

Eisaku Sasaki
1st Wireless Access Solutions Division
NEC Corporation
211-8666, Japan
sasaki-e@nec.com

2021 IEEE 94th Vehicular Technology Conference (VTC2021-Fall) | 978-1-6654-1368-8/21/$31.00 ©2021 IEEE | DOI: 10.1109/VTC2021-FALL52928.2021.9625460

***Abstract*—This work proposes and explores the use of probabilistic shaping for the non-orthogonal multicarrier spectrally efficient frequency division multiplexing (SEFDM) system. The system design considers the reverse concatenation architecture which cascades the constant composition distribution matching (CCDM) algorithm together with soft-decision forward error correction (SD-FEC)-LDPC code for the probabilistic shaping scheme. The non-orthogonal signalling is implemented by discrete Fourier transform (DFT)-based SEFDM modulation with matched filtering demodulation and advanced interference cancellation detection. The high achievable spectral efficiency, low computation complexity and reliability make SEFDM a good candidate for multicarrier signalling for beyond 5G communications. By adding extra shaping gain and flexibility of rate adaptation, the combination of two capacity-achieving techniques provides significant insight of further performance improvement. In this paper, we investigate the performance of the proposed probabilistically shaped-SEFDM (PS-SEFDM) system with regular QAM constellations. The presented results of the proposed system show less required power and bandwidth saving compared to OFDM when achieving the same error performance and same spectral efficiency.**

***Index Terms*—probabilistic shaping, data rate, non-orthogonal signalling, spectral efficiency**

I. Introduction

The beyond-5G and the envisioned sixth-generation (6G) networks are expected to move further to the ubiquitous connectivity for ultra-massive communications. From the physical layer aspect, spectrum scarcity and energy constraints have always been problems. To tackle such problems, signalling formats with higher spectral efficiency and better transmission reliability are required.

Spectrally efficient signalling techniques have been proposed and studied for new generations of communications other than orthogonal frequency division multiplexing (OFDM) as used in LTE and specified for 5G NR [1]. In general, these signalling methods are designed to be implemented in either the frequency-domain or the time-domain. The frequency-domain signalling approaches reduce the out-of-band (OOB) power emission of the waveforms. This can be achieved by means of windowing the time-domain symbols or pulse shaping/filtering techniques, with associated technologies including filter bank multi-carrier (FBMC), universal filtered multi-carrier (UFMC) and generalized frequency division multiplexing (GFDM). Alternatively, the non-orthogonal signalling formats improves the spectral efficiency by violating the signal orthogonality on which OFDM is based. The time-domain compression, termed as multi-stream faster than Nyquist (FTN), is known to offer up to 25% data rate increase without error performance degradation [2]. The spectrally efficiency frequency division multiplexing (SEFDM) exploits a similar idea in the frequency domain to the multiple subcarriers. SEFDM was first proposed in [3] in 2003 and has been studied and experimentally tested in optical, wireless, Visible light communications (VLC) and radio-over-fibre systems [4] [5], offering data rate increase by up to 40% with maintained error performance, at the expense of small power penalty and added complexity.

Sharing the same goal of approaching Shannon limit as non-orthogonal signalling, non-uniform signalling techniques have attracted great attention in academia and industry over the past two decades. Typical non-uniform approaches are based on constellation shaping as means of capacity-achieving methods by optimising the constellation design. Two existing techniques, geometric shaping and probabilistic shaping, were proposed and proven to offer large shaping gains, while reducing signal-to-noise ratio (SNR) to reach a certain data rate. Herein, probabilistic shaping achieves a higher capacity for Gaussian channels by approximating the Gaussian distribution among the occurrence probability distribution of the transmitted symbols. In particular, the ultimate shaping gain that can be achieved by probabilistic shaping is up to 1.53 dB (i.e. $\pi e/6$) as the modulation dimension approaches infinity [6].

To implement a probabilistic shaping system, a distribution matching (DM) encoder is used, which encodes the input bit stream to symbols with a target occurrence probability distribution. The first distribution matcher for noisy channels was implemented by a prefix-free code, proposed by G. Forney in 1984 [7]. Research on probabilistic shaping for non-uniform signalling mainly focused on designs of coded-modulation schemes and optimisations of the probability distribution to achieve higher shaping gains [8] [9] till the invention of the reverse concatenation architecture in [10] in 2015. This was followed by the proposal of classical constant composition distribution matching (CCDM) algorithm in 2016 [11]. Afterwards, gains achieved using probabilistic shaping

978-1-6654-1368-8/21/$31.00 ©2021 IEEE

resulted in increased interest, with investigations emerging in various communication systems. Probabilistic shaping has been widely used in coherent optical transmission systems to improve the capacity as well as to overcome the nonlinearity [12] [13]. There are also studies in wireless communications using probabilistic shaping for multicarrier signallings, such as OFDM [14] and the non-orthogonal FTN [15].

Coded-SEFDM systems have been investigated in [16] by using low-density parity-check (LDPC) coding, showing the advantages of bandwidth saving and less power requirement when preserving the same bit error rate (BER) relative to OFDM. Inspired by the works on coded-SEFDM and coded-modulation based probabilistic shaping, in this paper, we propose a novel system of non-orthogonal multicarrier SEFDM with probabilistic shaping. Specifically, we employ the reverse concatenation architecture [10] for the probabilistic shaping encoding/decoding with the CCDM algorithm [11] and LDPC coding [17]. An iterative detector (ID) is designed and employed to mitigate the interference resulted from the non-orthogonality of SEFDM. Performance comparison of the proposed system is investigated relative to the OFDM scheme under fixed spectral efficiencies by adjusting other parameters such as bandwidth compression level, coding rate and probabilistic shaping rate. Theoretical analysis of the achievable spectral efficiency is provided for different modulation schemes. Simulation results show the advantages of the proposed PS-SEFDM system compared to OFDM in terms of less required power while achieving the same error performance and saved bandwidth.

The rest of the paper is organised as follows: section II describes the basic concepts of SEFDM and probabilistic shaping scheme; section III details the transceiver structure and addresses the key metric—the achievable spectral efficiency that is held the same for the performance comparison; then in section IV, simulation results are discussed to show the system performance; finally, section V draws the conclusion.

II. Modulation Basics

A. SEFDM: flexible spectrally efficient waveform compression

SEFDM is a non-orthogonal multicarrier modulation scheme based on the idea of compressing the subcarrier frequency separation. Relative to OFDM, SEFDM deliberately violates the orthogonality to either reduce the occupied bandwidth to maintain the same transmission data rate, known as Type-I SEFDM, or to achieve a higher data rate within the same bandwidth, i.e. Type-II SEFDM [18]. In this work, we employ Type-I SEFDM to obtain a certain data rate. Despite the non-orthogonality, the signal processing in SEFDM is similar to that of OFDM. Therefore, the modulation/demodulation in SEFDM can be implemented efficiently by means of modified inverse fast Fourier transform (IFFT) and fast Fourier transform (FFT), respectively, as introduced in [19]. The difference between OFDM and SEFDM may be characterised by the bandwidth compression factor α (α = 1 for OFDM and < 1 for SEFDM), which determines $(1-\alpha) \times 100\%$ bandwidth saving achieved by SEFDM in comparison to OFDM for the same transmission speed. The discrete-time SEFDM symbol at the k^{th} time sample can be expressed as:

$$X[k] = \frac{1}{\sqrt{Q}} \sum_{n=0}^{N-1} s_n \cdot e^{j2\pi nk\alpha/Q}, \quad (1)$$

where $\mathbf{s} = [s_0, s_1, ..., s_{N-1}]$ is the incoming M-ary quadrature amplitude modulation (M-QAM) signal vector for N subcarriers and Q represents the total number of discrete-time samples in one SEFDM symbol. The factor $1/\sqrt{Q}$ is for the purpose of normalisation.

B. Probabilistic shaping with variable transmission rate

As pointed out in the introduction, probabilistic shaping exploits a symmetric occurrence distribution among the constellations of transmitted symbols to maximise the data rate for a given average power. The amplitude shaping based reverse concatenation architecture introduced in 2015 [10] combines shaping and coding in one scheme. Overall, at the transmitter side, the probabilistic shaping scheme can be seen as an encoder that converts the input random binary data to a shaped sequence with a target probability distribution based on the probabilistic shaping rate R_{ps}. Such architecture cascades the distribution matcher with FEC encoding and the probabilistic shaping decoder executes the inverse operations. The simplified structure is given in Fig.1 by showing only the key modules of the scheme. Herein, the distribution matcher performs shaping setting each symbol amplitude to match the occurrence probability distribution of the transmitted symbols to a set target probability.

Fixed-to-fixed length distribution matching techniques, employed regularly for probabilistic shaping, and the conventional single-composition arithmetic coding-based CCDM algorithm [11] is used in this work. With this technique, a negligible rate loss can be achieved through using relatively large input data length, as reported and thoroughly studied in an optical communications setting in [20]. As initially discussed in [11], the transmission rate is determined by the probability distribution of the symbols for specified power constraints. To approach the Shannon capacity limit of an additive white Gaussian noise (AWGN) channel, Gaussian-like distributions are considered. Specifically, the Maxwell-Boltzmann distribution, with a probability mass function given by $P_X(x) = e^{-\lambda x^2} / \sum_{x' \in X} e^{-\lambda x'^2}$ for any $x \in X$ with parameter λ, is found to be the optimal distribution for the occurrence probability of transmitted symbols in AWGN channels [9]. Therefore, for a given base constellation and transmission data rate, the average energy of shaped symbols with Maxwell-Boltzmann distribution can be minimised, as will be discussed in section IV.

To clarify, the FEC coding integrated with the distribution matching and inverse distribution matching (invDM) in this scheme is to enable data rate adaptation and to gain higher capacity. Moreover, the improved symbol error rate (SER) achieved by FEC coding also guarantees the invDM; since

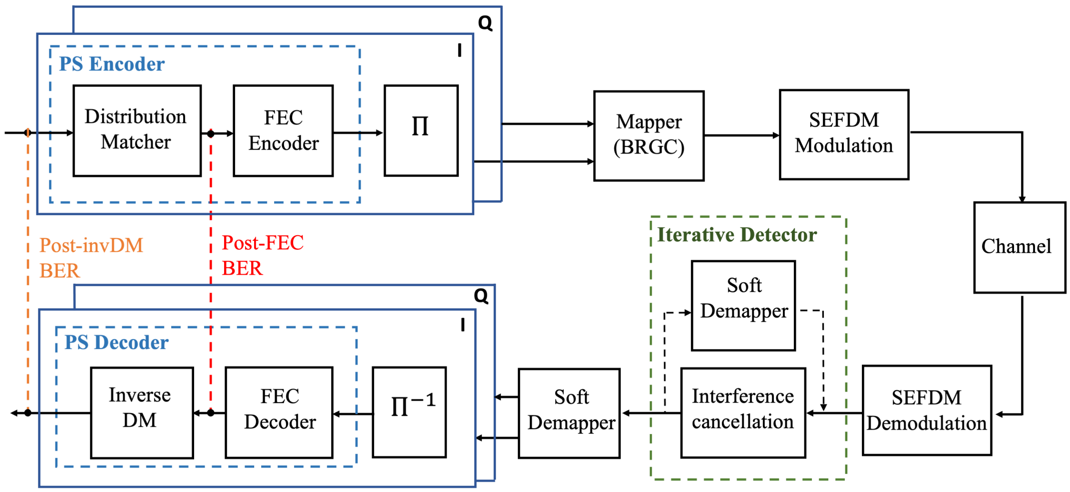

Fig. 1. Functional simplified block diagram of probabilistically shaped SEFDM system with iterative detection and LDPC coding.

the invDM only works at sufficient low SER to match the shaped symbols back into the input bits. To be precise, in this work we investigate both the post-FEC BER and post-invDM BER to present more practical results of error performance.

III. System Modelling

A. Transmitter Structure

The block diagram of the proposed probabilistically shaped-SEFDM (PS-SEFDM) system is depicted in Fig.1. The transmitter is constructed from two parallel encoders, followed by the concatenation of an interleaver, a bit-mapper and a SEFDM modulator. In this system model, we employ the one-dimensional probabilistic shaping followed by the binary reflected gray code (BRGC) mapper to generate pulse amplitude modulation (PAM) symbols. Two parallel probabilistic shaping functions are performed to generate the in-phase and quadrature components of a two-dimensional QAM.

At the transmitter, a stream of binary data $\mathbf{b} \in \{0,1\}$ feeds the probabilistic shaping encoder. The incoming binary sequence is framed into blocks of k bits. In the distribution matcher, each block of bit sequence is transformed into $n(m-1)$ bits corresponding to a block of amplitude sequence $\mathcal{A} \in \{0,1\}^{n(m-1)}$ with desired occurrence probability distribution, giving the DM rate $R_{DM} = k/n$, where $m = \log_2\sqrt{M}$ is determined by the constellation cardinality of M-QAM. In this work, we use standardized LDPC code [17] as the FEC, with codeword length n_c = 64,800 and coding rate $R_{fec} = (n_c - n)/n_c$. Since LDPC is a systematic binary code, in this procedure only the n parity bits are extracted to generate the sign sequence $\mathcal{S} \in \{0,1\}^n$. Although the information bits are discarded after encoding, the same information is kept in $\mathcal{A}$ for the decoding at the receiver side. The output nm bits of the probabilistic shaping encoder is obtained by concatenating the amplitude sequence $\mathcal{A}$ and the sign sequence $\mathcal{S}$.

Then, the BRGC maps the shaped bits to PAM symbols as one of the quadrature components of M-QAM. It is worth noting that the BRGC allows the probability distribution to be reserved when the Cartesian product of the two real-valued PAM constellations is exploited.

The probabilistically shaped QAM symbols are split into $N = 4$ parallel streams and modulated to N non-orthogonal SEFDM subcarriers using the IFFT-based method as mathematically described in section II.A and detailed in [19]. The SEFDM symbols are passed through an AWGN channel.

B. Receiver Structure

At the receiver side, SEFDM demodulation using modified FFT based matched filters [21] is adopted, however, unlike OFDM, the non-orthogonality of SEFDM with its self-introduced ICI would result in significant degradation of error performance unless appropriately mitigated. To this end, we utilise the iterative detector proposed in [22] to perform the interference cancellation and to recover the transmitted symbols with minimal error rate degradation. The dashed line, within the iterative detector block of Fig.1, indicates the feedback process that uses the subtraction results from the last iteration to update the new ICI information, according to the number of iterations set by the model. The constellation diagrams given in Fig.2 show the effectiveness of the iterative detector using SEFDM (α =0.8) as an example. For uniformly distributed SEFDM and PS-SEFDM, the 16-QAM constellation turns from (b) to (c) and from (e) to (f) after 5 iterations, respectively. The same study has been done with SEFDM (α =0.67) obtaining symbol recovery after 20 iterations. The constellation diagram is not given for space limitations. The output detected symbols are then passed to the soft demapper to generate soft bits, i.e. the *a posteriori* log-likelihood ratios (LLR). After the de-interleaving, the soft bits are fed to the probabilistic shaping decoder, in particular, to the FEC decoder so as to generate the encoded bits for the next iterations of the decoding. Herein we set 50 iterations for the LDPC decoder to achieve sufficiently low SER to make invDM perform the de-matching process.

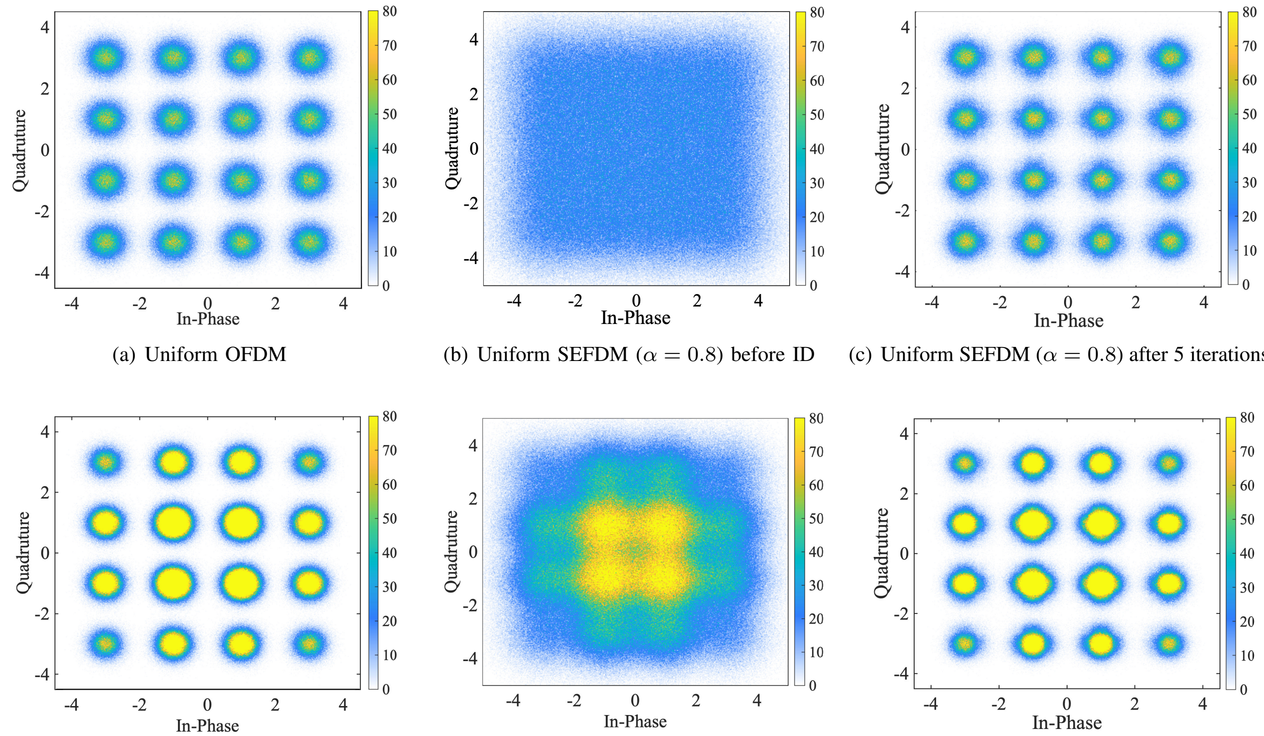

(a) Uniform OFDM (b) Uniform SEFDM ($\alpha = 0.8$) before ID (c) Uniform SEFDM ($\alpha = 0.8$) after 5 iterations

(d) PS-OFDM (e) PS-SEFDM ($\alpha = 0.8$) before ID (f) PS-SEFDM ($\alpha = 0.8$) after 5 iterations

Fig. 2. Constellation diagram for the received 16-QAM symbols at E_b/N_0 =12 dB.

C. Achievable Spectral Efficiency

For the proposed system, considering the probabilistic shaping rate R_{ps} and SEFDM compression factor α, the spectral efficiency can be expressed by

$$\eta = \frac{\log_2 M \times R_s \times R_{ps}}{\alpha \times B}, \tag{2}$$

where M is the constellation cardinality, B represents the occupied bandwidth, R_s denotes the SEFDM symbol rate. For M-QAM symbols the probabilistic shaping rate is determined by the DM rate and the FEC code rate as detailed in [20] for $\mathbf{n}$-dimensional constellations. In this work, regular M-QAM is adopted and the corresponding one-dimensional constellation is used as the base constellation for probabilistic shaping. For the case of 16-QAM, $M = 16$ and therefore the associated PAM-4 constellation points are $\{\pm 1, \pm 3\}$, where the number of amplitude levels $m = 2$. Consequently, the condition of the FEC code rate R_{fec} is given by

$$R_{fec} = \frac{n_c - n}{n_c} \geq \frac{m-1}{m}. \tag{3}$$

Thus, the smallest value of R_{fec} available for probabilistically shaped 16-QAM is 1/2.

IV. Performance Investigations

To evaluate the error performance of the proposed PS-SEFDM system, we carried out numerical simulations for both SEFDM and OFDM with and without probabilistic shaping based on complete modelling of the system blocks shown in Fig.1. To compare fairly the performance of the PS-SEFDM scheme relative to OFDM as well as to uniformly distributed SEFDM, we investigate different signals achieving the same spectral efficiency. Specifically, systems are evaluated at spectral efficiency values of 3.33 bits/s/Hz and 3.75 bits/s/Hz in terms of BER performance and spectrum property; E_b/N_0 is used to measure the SNR for a fair comparison, due to the use of FEC coding and bandwidth compression. The required E_b/N_0 are assessed at post-FEC BER of 10^{-4} meanwhile the post-invDM BER of 10^{-3} approximately. For spectral efficiency η = 3.33 bits/s/Hz, the comparison is held for 16-QAM SEFDM (α = 0.8) and OFDM with and without probabilistic shaping. In this case, coded-OFDM with code rate R_c = 5/6 achieves the same spectral efficiency as coded-SEFDM with R_c = 2/3. To achieve the same spectral efficiency, the corresponding R_{ps} of the probabilistic shaping scheme is required to equal the R_c of the schemes without probabilistic shaping. For the η = 3.75 bits/s/Hz spectral efficiency case, we compare the PS-16-QAM-SEFDM, with two different compression factors α = 0.8 and α = 0.67, to the 32-QAM coded-OFDM.

Before assessing the BER performance, we study the constellation diagrams of the uniformly distributed and the probabilistically shaped symbols with the base constellation of 16-QAM as demonstrated in Fig.2. The simulations were conducted at E_b/N_0 = 12 dB, it can be seen that for both OFDM and SEFDM with probabilistic shaping, the constella-

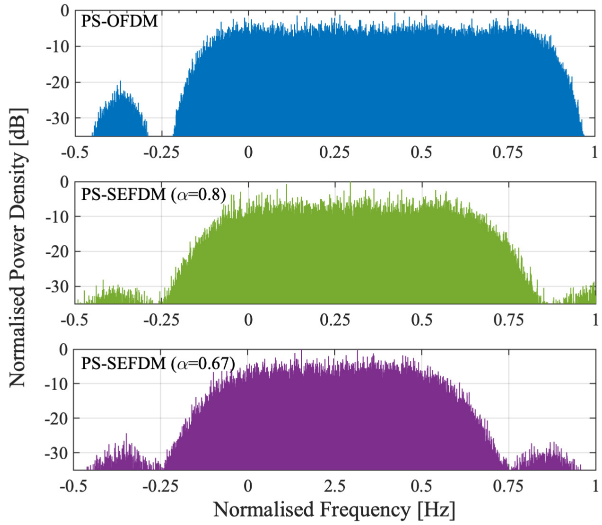

Fig. 3. Power spectrum comparison of PS-OFDM/-SEFDM (α = 0.8, 0.67).

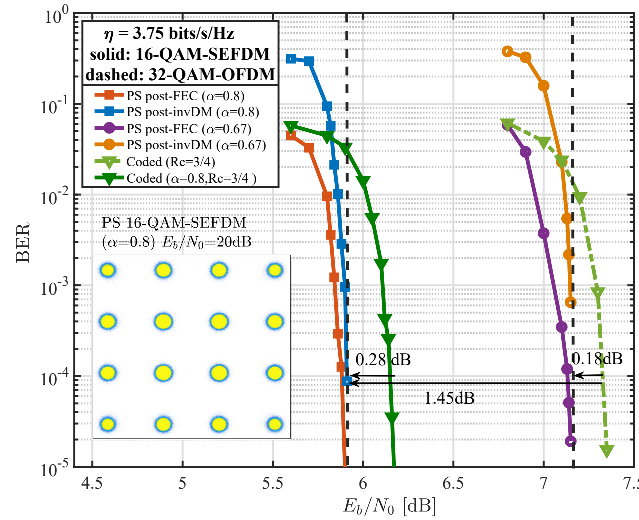

Fig. 5. η = 3.75 bits/s/Hz: BER performance of PS-SEFDM (α = 0.8, 0.67), coded-SEFDM (α = 0.8) and coded-OFDM.

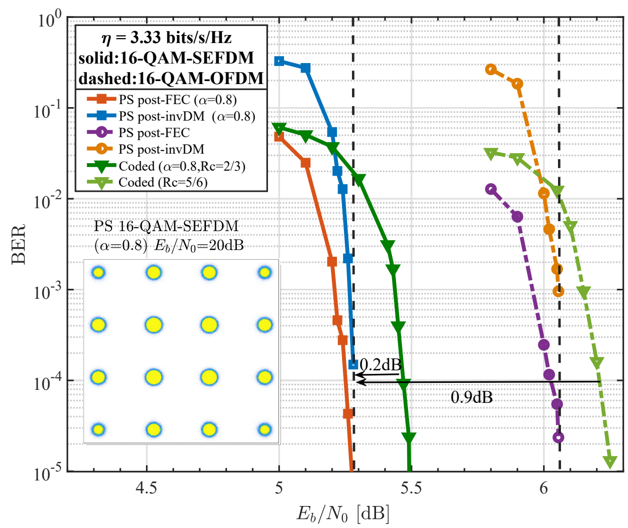

Fig. 4. η = 3.33 bits/s/Hz: BER performance of PS-SEFDM (α = 0.8), PS-OFDM, coded-SEFDM (α = 0.8) and coded-OFDM.

tion points with lower energy are transmitted more frequently as in the theory.

We conducted simulations for various spectral efficiencies and in this paper, only two groups of results are presented to illustrate the performance and advantages of using PS-SEFDM. The first group with 3.33 bits/s/Hz in Fig.4 shows the advantage of using SEFDM with probabilistic shaping and a lower coding rate relative to OFDM, specifically, 0.7 dB power advantage and 0.2 dB shaping gain. The total 0.9 dB gain of 16-QAM PS-SEFDM (α = 0.8) can be seen when compared to 16-QAM OFDM without probabilistic shaping. In all cases, the SEFDM signal has 25% bandwidth saving relative to the OFDM, noting the spectrum of the (α = 0.8) case of Fig.3. For the second group with spectral efficiency η = 3.75 bits/s/Hz, Fig.5 shows similar advantage of PS-SEFDM when α = 0.8. The 16-QAM PS-SEFDM achieves 1.45 dB power savings when compared to the uniformly distributed 32-QAM-SEFDM. For PS-SEFDM with α = 0.67 (bottom spectrum of Fig.3), which is lower than the Mazo limit (i.e. 0.8), there is a slight performance advantage as well as 50% bandwidth saving over the uniformly distributed 32-QAM OFDM. The constellation diagrams of 16-QAM PS-SEFDM (α = 0.8) at the high E_b/N_0 value of 20 dB, for the two different spectral efficiency values of 3.33 and 3.75 bits/s/Hz, are shown as insets in Fig.4 and Fig.5, respectively. These clearly indicate there will be no error floor behavior even at when the operation is almost noise free. The advantages obtained by using probabilistic shaping in AWGN environments are also predicted to be evidenced in realistic fading channels, which are the subject of ongoing studies now.

To conclude, the PS-SEFDM always outperforms non-shaped SEFDM and OFDM with the same spectral efficiency. When the same BER performance is obtained, the shaping procedure introduces extra shaping gain on top of the power advantage of SEFDM using lower coding rate [16] relative to OFDM. In addition, the probabilistic shaping scheme per se is limited by the DM rate considering the rate loss as well as the minimum FEC code rate as given in equation (3). The use of SEFDM with varying compression factor extends the flexibility of rate adaptation of probabilistic shaping scheme.

V. Conclusions

This work investigates a new idea to improve further the capacity of spectrally efficient multicarrier signals by applying probabilistic shaping to the SEFDM signals. In the system design, we employ the conventional fixed-length single-composition distribution matching algorithm and reverse concatenation probabilistic shaping architecture coupled with LDPC coding and iterative detector for interference cancellation. A fair comparison is held by maintaining fixed achievable spectral efficiency for SEFDM with and without probabilistic shaping with varying compression factor compared to OFDM. The error performance demonstrates significant shaping gains together with the power advantage relative to OFDM. Therefore, this technique advantageously results in transmission energy saving coupled with substantial bandwidth saving and allows flexible data rate adaptation, all at the expense of a limited increase in complexity.

ACKNOWLEDGEMENT

Xinyue Liu is grateful to NEC Laboratories Europe GmbH for part funding of her PhD studies through the NEC Laboratories Europe GmbH internship funding.

REFERENCES

[1] D. Rainnie, Y. Feng, and J. Bajcsy, "On capacity merits of Spectrally Efficient FDM," in *MILCOM 2015-2015 IEEE Military Communications Conference*. IEEE, 2015, pp. 581–586.

[2] J. E. Mazo, "Faster-than-Nyquist signaling," *Bell System Technical Journal*, vol. 54, no. 8, pp. 1451–1462, 1975.

[3] M. Rodrigues and I. Darwazeh, "A Spectrally Efficient Frequency Division Multiplexing based communications system," in *Proc. 8th Int. OFDM Workshop*, 2003, pp. 48–49.

[4] I. Darwazeh, H. Ghannam, and T. Xu, "The first 15 years of SEFDM: A brief survey," in *2018 11th International Symposium on Communication Systems, Networks Digital Signal Processing (CSNDSP)*, 2018, pp. 1–7.

[5] X. Liu, T. Xu, and I. Darwazeh, "Coexistence of orthogonal and non-orthogonal multicarrier signals in beyond 5G scenarios," in *2020 2nd 6G Wireless Summit (6G SUMMIT)*, 2020, pp. 1–5.

[6] G. Forney and L.-F. Wei, "Multidimensional constellations. i. introduction, figures of merit, and generalized cross constellations," *IEEE Journal on Selected Areas in Communications*, vol. 7, no. 6, pp. 877–892, 1989.

[7] G. Forney, R. Gallager, G. Lang, F. Longstaff, and S. Qureshi, "Efficient modulation for band-limited channels," *IEEE Journal on Selected Areas in Communications*, vol. 2, no. 5, pp. 632–647, 1984.

[8] G. D. Forney, "Trellis shaping," *IEEE Transactions on Information Theory*, vol. 38, no. 2, pp. 281–300, 1992.

[9] F. Kschischang and S. Pasupathy, "Optimal nonuniform signaling for Gaussian channels," *IEEE Transactions on Information Theory*, vol. 39, no. 3, pp. 913–929, 1993.

[10] G. Böcherer, F. Steiner, and P. Schulte, "Bandwidth efficient and rate-matched low-density parity-check coded modulation," *IEEE Transactions on Communications*, vol. 63, no. 12, pp. 4651–4665, 2015.

[11] P. Schulte and G. Böcherer, "Constant composition distribution matching," *IEEE Transactions on Information Theory*, vol. 62, no. 1, pp. 430–434, 2016.

[12] T. Fehenberger, G. Böcherer, A. Alvarado, and N. Hanik, "LDPC coded modulation with probabilistic shaping for optical fiber systems," in *Optical Fiber Communication Conference*. Optical Society of America, 2015, pp. 1–3.

[13] F. Buchali, G. Böcherer, W. Idler, L. Schmalen, P. Schulte, and F. Steiner, "Experimental demonstration of capacity increase and rate-adaptation by probabilistically shaped 64-QAM," in *2015 European Conference on Optical Communication (ECOC)*, 2015, pp. 1–3.

[14] Y. C. Gültekin, W. J. van Houtum, A. G. C. Koppelaar, F. M. J. Willems, and W. J. van Houtum, "Enumerative sphere shaping for wireless communications with short packets," *IEEE Transactions on Wireless Communications*, vol. 19, no. 2, pp. 1098–1112, 2020.

[15] W. Kang, H. Che, and K. Zhu, "Precoding optimization for Faster-than-Nyquist signaling with probabilistic shaping," *IEEE Transactions on Vehicular Technology*, vol. 69, no. 10, pp. 11 470–11 478, 2020.

[16] H. Ghannam and I. Darwazeh, "SEFDM over satellite systems with advanced interference cancellation," *IET Communications*, vol. 12, no. 1, pp. 59–66, 2017.

[17] *Second Generation Framing Structure, Channel Coding and Modulation Systems for Broadcasting, Interactive Services, News Gathering and Other Broadband Satellite Applications; Part 1 (DVB-S2)*, ETSI Standard EN 302 307-1 v1.4.1, Nov.2014.

[18] T. Xu and I. Darwazeh, "Non-orthogonal narrowband internet of things: A design for saving bandwidth and doubling the number of connected devices," *IEEE Internet of Things Journal*, vol. 5, no. 3, pp. 2120–2129, 2018.

[19] S. Isam and I. Darwazeh, "Simple DSP-IDFT techniques for generating Spectrally Efficient FDM signals," in *2010 7th International Symposium on Communication Systems, Networks Digital Signal Processing (CSNDSP 2010)*, 2010, pp. 20–24.

[20] G. Böcherer, P. Schulte, and F. Steiner, "Probabilistic shaping and forward error correction for fiber-optic communication systems," *Journal of Lightwave Technology*, vol. 37, no. 2, 2019.

[21] P. N. Whatmough, M. R. Perrett, S. Isam, and I. Darwazeh, "VLSI architecture for a reconfigurable Spectrally Efficient FDM baseband transmitter," in *2011 IEEE International Symposium of Circuits and Systems (ISCAS)*, 2011, pp. 1688–1691.

[22] T. Xu, R. C. Grammenos, F. Marvasti, and I. Darwazeh, "An improved fixed sphere decoder employing soft decision for the detection of non-orthogonal signals," *IEEE Communications Letters*, vol. 17, no. 10, pp. 1964–1967, 2013.